JOURNAL OF MATERIALS SCIENCE **36** (2001) 5481–5486

Synthesis and characterisation of hydroxy/fluoroapatite solid solution

I. MANJUBALA
Materials Science Centre, Department of Nuclear Physics, University of Madras, Guindy Campus, Chennai 600 025, India
E-mail: imc48@hotmail.com

M. SIVAKUMAR
Biomaterials Division, Central Leather Research Institute, Adyar, Chennai 600 020, India

S. NAJMA NIKKATH
Materials Science Centre, Department of Nuclear Physics, University of Madras, Guindy Campus, Chennai 600 025, India

Hydroxyapatite (HA) and fluoroapatite (FHA) have been widely investigated as bone substitute and replacement materials. We report here the preparation of hydroxy/fluoroapatite solid solution using wet chemical precipitation method via brushite hydrolysis. Various amounts of sodium fluoride (1–5 mol%) were added during the preparation of hydroxyapatite to form hydroxy/fluoroapatite solid solution. The various experimental techniques like XRD, DTA, TGA, FT-IR and Vicker's hardness measurements were used to characterize the synthesized powders. Thermal analysis of the samples shows only the decomposition reaction of residues formed and the corresponding weight loss due to these reactions. The XRD data of all the samples calcined at 900°C shows well defined peaks of hydroxyapatite and fluoroapatite. The merging of (211) and (112) peak of apatite lattice in the FHA pattern indicates the formation of hydroxy/fluoroapatite solid solution. The decrease in the a-axis of HA lattice parameter indicates the substitution of F^- ion in the OH^- site of HA lattice. The FT-IR spectroscopic studies of the samples confirms the substitution of the F^- ion in the OH^- site of the HA lattice. The Vicker's hardness measurement shows that the hardness value of hydroxy/fluoroapatite solid solution is greater than the hydroxyapatite.

1. Introduction

Synthetic hydroxyapatite (HA) has been used extensively as bone implant materials due to their identical chemical composition and high biocompatibility with natural bone [1–3]. The inorganic matrix component of bone is based on hydroxyapatite $Ca_{10}(PO_4)_6(OH)_2$ doped with different quantities of cations like Na^+, K^+ and Mg^{2+} which occupy Ca^{2+} sites and anions such as CO_3^{2-}, SO_4^{2-} and F^- substituting OH^- groups. These dopants especially F^- exercise a great influence on the physical and biological properties of the material [4, 5]. Fluoride is an essential trace element required for normal dental and skeletal development. It has been shown that the presence of fluoride has certain beneficial effects in increasing the quantity and quality of bone formation in the body [6]. Thus, the bone mineral produced by fluoroapatite is less susceptible to dissolution and possibly resorption.

Since fluoride is well known for caries prevention and for the treatment of osteoporosis, fluoroapatite has been widely investigated [7–9]. Stoichiometric fluoroapatite has fluorine content of 3.77 wt% but the fluorine content of human bone is less than 1 wt%. Implant materials should not exhibit notably higher fluorine concentration otherwise toxic reactions cannot be avoided [10, 11]. There are various fluoridated apatites with different degrees of fluoridation, $Ca_{10}(PO_4)_6(OH)_{2-2x}F_{2x}$ (x is the degree of fluorination, $x = 0$ hydroxyapatite, $x = 1.0$ fluoroapatite, $0 < x < 1$ forms hydroxy/fluoroapatite solid solution). Fluorine tends to increase the crystal size due to the increased crystal growth rate, resulting in decreased strain on the apatite lattice and increased stability of the apatite structure. At lower degrees of fluoridation the apparent solubility decreases markedly. The mechanism by which fluoride reduces the solubility of hydroxyapatite has been investigated intensively [12–14].

Numerous synthesis methodologies of HA are known, such as precipitation, solid state synthesis, hydrolysis, hydrothermal and sol-gel methods. Among them precipitation method appears to be the most commonly used [15]. Precipitation method and sol-gel methods have been used for preparation of homogeneous fluoroapatite. Heterogeneous fluoroapatite have been prepared and also been reported in the form of functional gradient form [16, 17]. The depth profile of

fluorine varies continuously in heterogeneous system rather than in homogeneous system in which a solid solution of various degree of fluoridation is obtained. We have already reported the formation of homogeneous system of hydroxy/fluoroapatite solid solution using the HA obtained from Indian corals and reacting it with sodium fluoride at high temperature [18]. The aim of this study is to achieve the direct formation of hydroxy/fluoroapatite solid solution by wet chemical precipitation method via brushite hydrolysis procedure with varying degree of fluoridation.

2. Materials and methods

2.1. Material preparation

Analytical grade calcium acetate [$Ca(CH_3COO)_2$] (CDH, India) and orthophosphoric acid [H_3PO_4] (Qualigens, ExcelaR@, India) were used as starting material for calcium and phosphorus precursors. The preparation of hydroxyapatite via brushite hydrolysis is as follows: A solution of calcium acetate (1.0 M) in deionized distilled water was prepared and the pH was adjusted to 9 with concentrated NH_4OH and thereafter diluted. The calcium solution stirred continuously at room temperature and the phosphoric acid (0.6 M) was added drop by drop for 30 to 35 min to produce a gelatinous precipitate. The precipitate was stirred continuously at 80°C and the pH was maintained at 9 by adding additional amount of concentrated NH_4OH solution. A part of the precipitate was filtered, (sample coded as HA-P) washed and dried. The rest of the precipitate was hydrolysed at 80°C for 24 h and then filtered (sample coded as HA-I). The precipitates were washed twice with distilled water, dried at 90°C overnight. For the formation of hydroxy/fluoroapatite solid solution, sodium fluoride (1, 3, 5 mol%) was added to the calcium precursor solution and the process was carried out. The precipitates were filtered after 24 h of hydrolysis and the powders were used for analysis. The dried powders were calcined at 900°C for 12 h in air atmosphere and used for further analysis.

2.2. Characterization

The synthesized powders were subjected to various investigations using the experimental techniques like XRD (Seifert, XRD 3000 Germany), DTA (Perkin Elmer PE-7 Series, USA), TGA (Perkin Elmer PE-7 Series, USA), FT-IR (Nicolet Impact FTIR 4000, Japan) and Vickers microhardness tester (Reichert). X-ray powder diffraction (XRD) data were collected from $2\theta = 20°$ to 60° using the monochromatic Cu K_α radiation at the step of 0.02 degrees with a count time of 1 sec at each step. The crystalline phases and cell dimensions were found from the diffraction profiles. The average grain size was estimated from the FWHM values of the theoretically fitted diffraction profiles using Scherrer formula [19]. The average grain size (t) of the particles are calculated using the formula $t = 0.9\lambda/\beta \cos\theta$ where λ is the wavelength of the source used (here $\lambda = 0.15405$ nm), β is the full width at the half maximum intensity (FWHM) and θ is the corresponding diffracting angle. The cell parameters were calculated using the least square fitting method of CELN program. Fourier transform infrared (FT-IR) spectroscopic data were taken to find the molecular bonding and the substitutions of anions and cations in HA. FT-IR spectra were obtained in the region 400–4000 cm^{-1} of the powdered samples in the pellet form mixed with spectroscopic grade KBr. Differential thermal analysis (DTA) and thermogravimetric analysis (TGA) were carried out in the temperature range of 50° to 1200°C and 50° to 900°C respectively in a stream flow of nitrogen gas with a heating rate of 10°C/min.; α-alumina powder was used as reference material for DTA measurement. Disc shaped specimen of dimensions 1 cm in diameter and 0.2 cm in thickness were prepared by applying a pressure of 80 MPa using a hydraulic press and the specimens were sintered at 1200°C in air for 2 h. The sintered specimens were polished using an automated Motopol 2000 polisher and used for microhardness measurement. The indentation diagonals were measured with a help of an optical Leica microscope attached to the microhardness tester. The Vicker's hardness values were

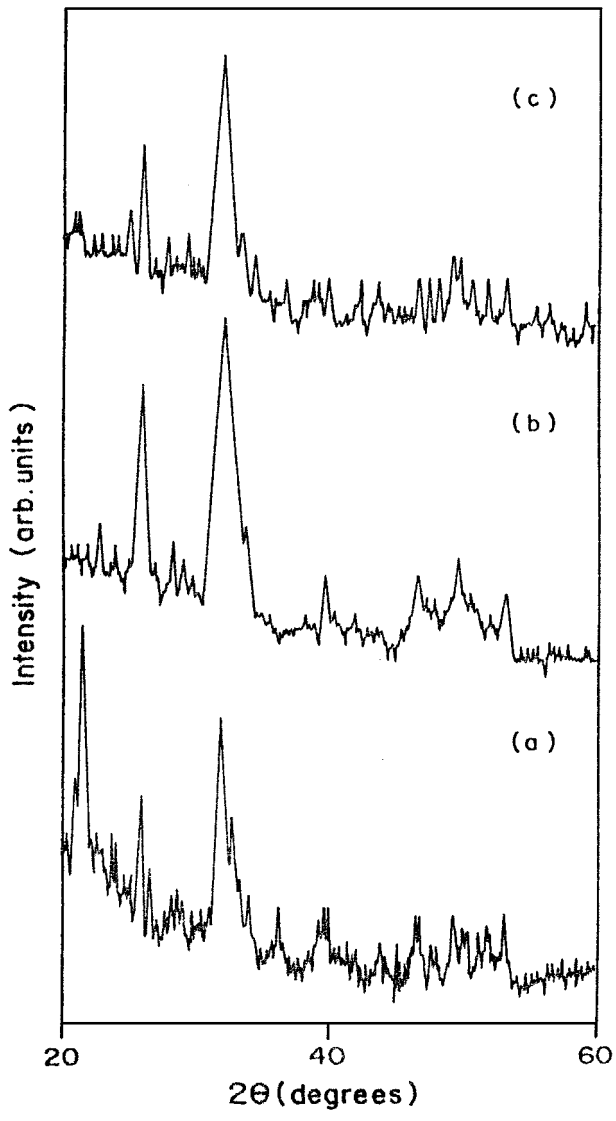

Figure 1 X-ray diffraction pattern of (a) HA filtered immediately after precipitation (HA-P) powder (b) HA filtered after incubation of 24 h (HA-I) and (c) fluoroapatite filtered after 24 h of incubation (5FHA).

obtained using the relation $H_v = 1854.4P/d^2$, where P is the indentation load in gram-force and d is the indentation diagonal in micrometers [20].

3. Results and discussion

The x-ray diffractograms (XRD) of the precipitated dried powders of HA-P, HA-I and 5FHA is shown in Fig. 1. The broader peak appears at the main regions of HA (31.5°) indicating the microcrystalline nature of the powders. These powders exhibit low degree of crystallinity, which is known to be a typical characteristic of calcium phosphate synthesized by the wet precipitation method [21]. The XRD pattern of HA-I and 5FHA shows peaks at 26° and 31°, which are the characteristic peaks of HA. The HA-P powder pattern shows a distinct peak at 22°, different from HA peaks. To improve the crystallinity and to analyse the phases formed, the powders were calcined at 900°C. The calcined powders show a substantial increase in intensity and an associated drop in the peak width that corresponds to an increase in crystallinity. The effect of calcination may increase the overall crystal lattice size. However, the calcination temperature below 1000°C may be ideal, as the formation of TCP has been reported if the temperature reaches 1000°C and above [22]. Hence to identify the phases formed and differentiate the peaks, the powders were calcined at 900°C for 12 h in air atmosphere. The XRD patterns of HA-P and HA-I after calcination shows well defined peaks as shown in Fig. 2. The pattern of HA-P does not correspond to HA peaks, they were identified as β-tricalcium phosphate (β-TCP) peaks and indexed corresponding to the standard values (JCPDS 9-169 [23]). The pattern of HA-I shows the characteristic peaks of HA along with TCP peak (marked as •). The presence of TCP indicates that the hydrolysis of HA precursor precipitate has not yet completed and shows that calcium deficient HA was formed which decomposes to β-TCP below 900°C.

The XRD patterns of (1–5 mol%) sodium fluoride doped HA i.e. 1FHA, 3FHA and 5FHA calcined at 900°C are shown in Fig. 3. In all the samples the TCP phase is absent and highly crystalline HA is formed.

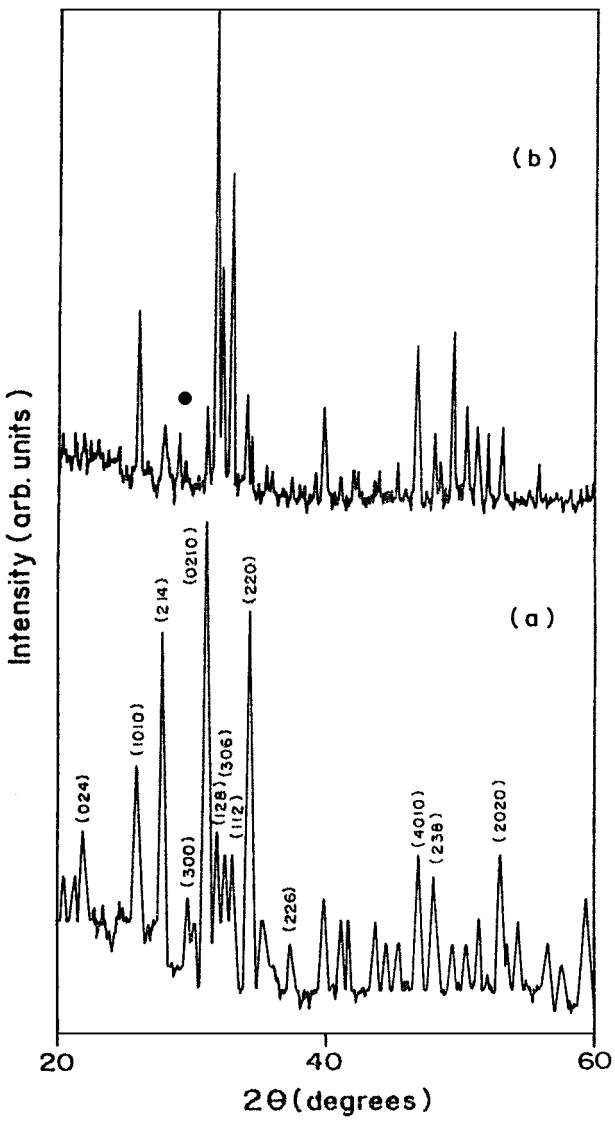

Figure 2 X-ray diffraction pattern of (a) HA-P and (b) HA-I samples after calcination at 900°C: (•—β-TCP peaks).

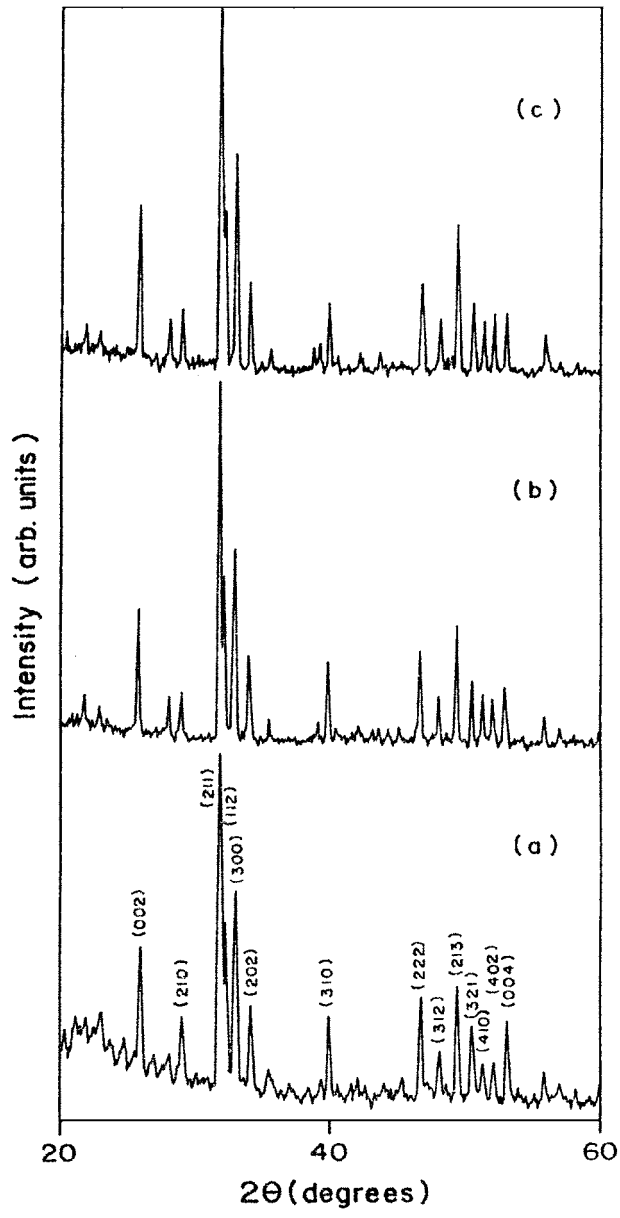

Figure 3 X-ray diffractograms of (a) 1FHA (b) 3FHA and (c) 5FHA apatites incubated for 24 h and calcined at 900°C.

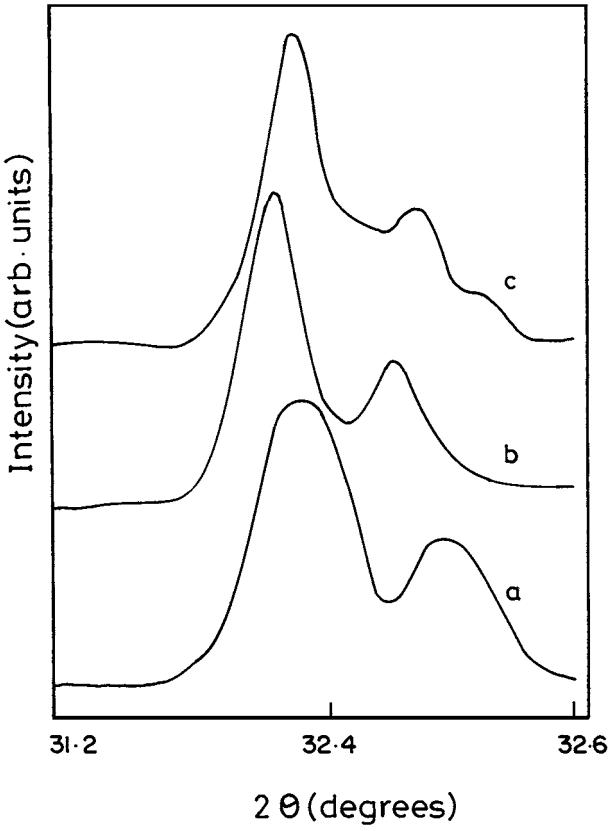

Figure 4 Expanded XRD patterns in the region of (211) and (112) peak. (a) 1FHA (b) 3FHA and (c) 5FHA apatites.

The (211) and (112) peaks at 31.8° and 32.2° respectively of HA merges with each other as the fluorine content increases (Fig. 4). The effect of incubation period for the formation of FHA has been analysed in the 3FHA sample and the precipitates were filtered after 6, 12, 18 h of incubation period. The XRD pattern of these samples heated to 900°C is shown in Fig. 5. The XRD pattern of 3FHA after 6 h incubation as shown in Fig. 5a indicates the presence of TCP phase in FHA. The patterns of FHA hydrolysed for 12, 18 and 24 h (Figs 5b, c, and 3d) shows the formation of fluoroapatite without any TCP peaks.

The HA peaks were indexed according to the standard values (JCPDS 9-432 [24]) and analysed to obtain the *d*-spacing values. The substitution of fluorine in HA lattice is analysed from the shift of the HA peaks. The shift in (300) peak also indicates the decrease of *a*-axis of the HA lattice [25]. The (002) peak of FHA is shifted to left compared to HA and the (300) peak of FHA is shifted to right towards higher angle and this indicates the decrease of *a*-axis of HA lattice cell. The FWHM values and the average grain size of the materials are reported in Table I. The calculated *d*-spacing of the peaks

TABLE I Crystallite size of HA and FHA samples calcined at 900°C

Samples	FWHM	Average grain size (nm)
HA-I	0.0722	115
1FHA	0.0822	100
3FHA	0.0856	97
5FHA	0.0868	95

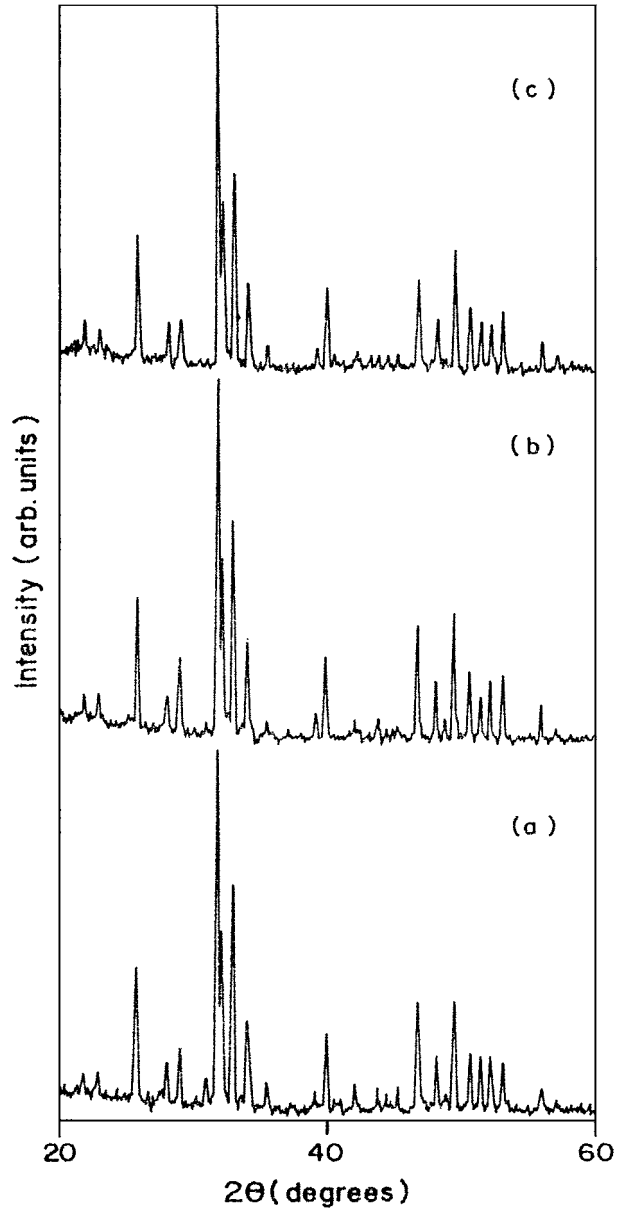

Figure 5 X-ray diffraction patterns of 3FHA apatite formed after (a) 6 (b) 12 and (c) 18 h of incubation after precipitation and calcined at 900°C.

coincides with literature values and the cell dimensions are listed in Table II.

The FT-IR spectra of HA-I, 3FHA and 5FHA samples are shown in Fig. 6. The hydroxyl bond stretch is observed at 3560 cm^{-1} without any drastic change in the peak position in all the samples, but the peak area decreases. As the fluorine substitutes at the hydroxyl site of the HA lattice, the hydroxyl band at 630 cm^{-1} disappears in both the samples. This confirms the formation

TABLE II List of cell parameters of HA and FHA samples calcined at 900°C calculated from the XRD data

Samples	*a* axis (Å)	*c* axis (Å)
JCPDS (9-432)	9.418	6.884
HA-I	9.440 ± 0.008	6.889 ± 0.004
1FHA	9.427 ± 0.005	6.909 ± 0.008
3FHA	9.412 ± 0.003	6.907 ± 0.006
5FHA	9.404 ± 0.005	6.908 ± 0.003

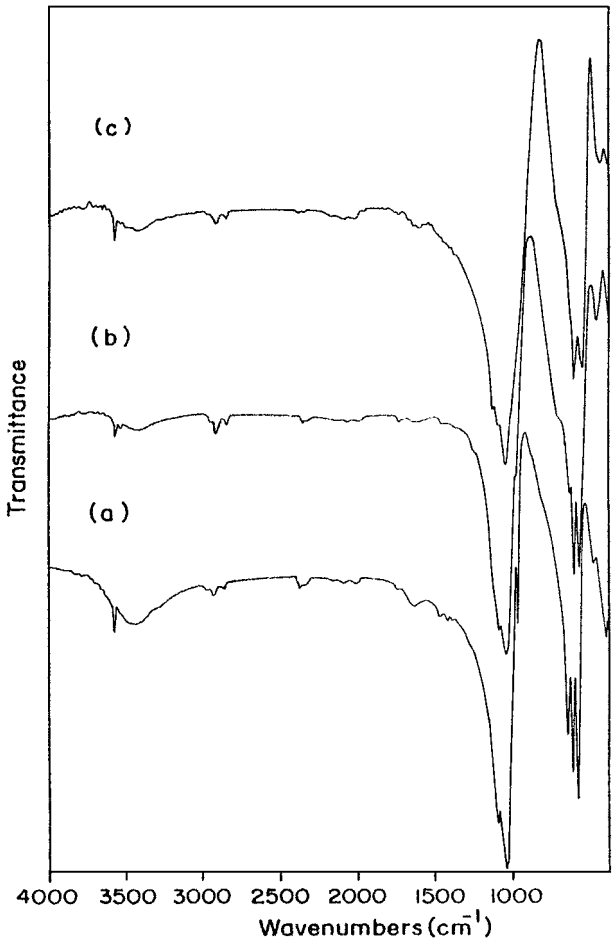

Figure 6 FT-IR spectra of (a) HA-I, (b) 3FHA and (c) 5FHA calcined samples.

of fluoroapatite in these samples. The vibrational bands of the phosphate ions are observed in all the samples. The phosphate band is observed at 602 and 566 cm^{-1}, but the resolution decreases in the fluoroapatite samples with the decrease in the peak area. The band around 1000 cm^{-1} appears as a triplet in pure HA with peaks well resolved at 1096, 1085 and 1056 cm^{-1}, but in the fluoroapatite samples the triplet resolution decreases and broadening takes place.

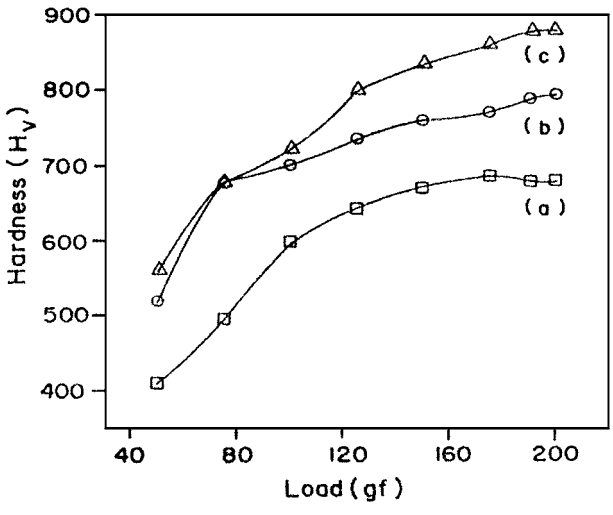

Figure 7 Vicker's hardness values plotted for (a) HA-I, (b) 3FHA and (c) 5FHA specimens sintered at 1200°C.

The DTA and TGA analysis of the samples HA-P, HA-I and 5FHA were carried out. An endothermic peak and the corresponding weight loss is observed in all the samples in the temperature range 120°–160°C due to the evaporation of the adsorbed water. In HA-P sample the decomposition of the residue and the ammonium salts is observed at 280°C and a small weight loss at 700°C showing the decomposition of calcium deficient apatite.

The Vicker's microhardness values of the samples HA-I, 3FHA and 5FHA are shown in Fig. 7 for various loads. The hardness of the HA and FHA samples sintered at 1200°C shows values better than 900°C calcined samples due to densification. The FHA samples show greater value of hardness than HA indicating that the fluorine imposes strength to the HA lattice.

4. Conclusion

Hydroxy/fluoroapatite solid solution with various concentration of fluorine were successfully prepared by wet chemical method and it is well characterised. It has been shown that sufficient hydrolysis at high temperature is necessary for the formation of pure apatites. The decrease in *a*-axis of the HA lattice parameter from the XRD result and the disappearance of the hydroxyl vibrational band in the FT-IR spectra confirms the fluorine substitution in the HA lattice.

Acknowledgements

The facilities made available under SAP and COSIST Schemes of University Grants Commission (UGC) of India are gratefully acknowledged. The authors are grateful to Prof. P. R. Subramanian for his constant support in this work.

References

1. M. JARCHO, C. H. BOLEN, M. B. THOMAS, J. BOBICK, J. F. KAY and R. M. DOREMUS, *J. Mater. Sci.* **11** (1976) 2027.
2. DEAN-MO LIU, *ibid.* **8** (1997) 227.
3. K. DE GROOT, *Biomaterials* **1** (1980) 47.
4. T. KANAZAWA, T. UMEGAKI, K. YAMASHITA, H. MONMA and T. HIRAMATSU, *J. Mater. Sci.* **26** (1991) 417.
5. L. L. HENCH, *J. Amer. Ceram. Soc.* **74** (1991) 1487.
6. J. CARSTEN and B. MARCO, *Biomaterials* **17** (1996) 2065.
7. F. C. M. DRIESSENS, *Nature* **243** (1973) 240.
8. E. C. MOREN, M. KRESAK and R. T. ZAHRADNIK, *Caries Res.*, **11** (1977) 142.
9. J. D. FEATHERSTONE, R. GLENA, M. SHARIATI and C. P. SHIELD, *J. Dent. Res.* **69** (1990) 634.
10. J. F. OSBORN and H. NEWESLEY, *Biomaterials* **1** (1980) 108.
11. U. PARTENFELDER, A. ENGEL and C. J. RUSSEL, *J. Mater. Sci. Mater. Med.* **4** (1993) 292.
12. J. A. GRAY, *J. Dent. Res.* **44** (1965) 497.
13. N. A. MIR and W. I. HIGUCHI, *Arch. Oral Biol.* **14** (1969) 901.
14. F. C. M. DREISSENS, *Nature* **243** (1973) 420.
15. N. ASOAKA, S. BEST, J. KNOWLES and W. BONFIELD, *Bioceramics* **8** (1995) 331.
16. M. OKAZAKI, H. TONDA, T. YANAGISAWA, M. TAIRA and J. TAKAHASHI, *Biomaterials* **19** (1998) 611.
17. M. OKAZAKI, Y. MAIKE, T. YANAGIASAWA, T. MATSUMOTO and T. TAKAHASHI, *ibid.* **20** (1999) 1421.

18. T. S. SAMPATH KUMAR, M. SIVAKUMAR, N. PRASANTH KUMAR, K. SENTHAMIL SELVI and K. PANDURANGA RAO, *Bull. Mater. Sci.* **8** (1995) 955.
19. B. D. CULLITY, "Elements of X-ray Diffraction," 2nd ed. (Addison Wesley, London, 1978).
20. E. L. WETZLAR, "A Guide for Working with the DURIMET Small Hardness Tester" (Ernst Leitz GmbH Wetzlar, Germany).
21. S. PUAJINDANETR, S. BEST and W. BONFIELD, *Brit. Ceram. Trans.* **93** (1994) 96.
22. S. W. K. KWEH, K. A. KHOR and P. CHEANG, *J. Mater. Process. Tech.* **89/90** (1999) 373.
23. JCPDS File No. 9-169 (TCP) (Joint Committee on Powder Diffraction Standards, Swathmore, PA, 1988).
24. JCPDS File No. 9-432 (HA) (Joint Committee on Powder Diffraction Standards, Swathmore, PA, 1988).
25. L. J. JHA, S. BEST, J. D. SANTOS and W. BONFIELD, *Bioceramics* **9** (1996) 165.

Received 19 May 2000
and accepted 19 July 2001